Low-Complexity Joint Range and Direction Estimation from Two-Way Multi-Carrier Phase Measurements

Johan Suárez, Kimmo Kansanen
Department of Electronic Systems, Norwegian University of Science and Technology, Trondheim, Norway
johan.suarez@ntnu.no, kimmo.kansanen@ntnu.no

***Abstract*—This paper proposes a low-complexity method for joint range and propagation direction estimation from two-way multi-carrier phase measurements collected by a linear antenna array, and processing them with a FFT-based algorithm.**

The proposed approach applies FFTs on the measured frequency-domain data in frequency and spatial dimensions to obtain initial delay and angle estimates, and then performs a gradient based structured search over propagation angles to improve the angular precision beyond what is provided by the FFT based estimate. Performing the latter only on the dominant peak of the impulse response allows for a low complexity search. The computational complexity is dominated by the FFT dimensions, and scales linearly with the number of antenna elements.

Simulation results demonstrate that the proposed method achieves near-optimal performance in both range and angle estimation. In particular, the estimator approaches the corresponding marginal Cramér–Rao bound of each parameter of interest at approximately -5 dB SNR for range estimation and 0 dB SNR for angle estimation.

***Index Terms*—Bluetooth Low Energy (BLE), channel sounding, direction finding, distance estimation, ranging, localization, phase-measurement**

I. Introduction

Joint estimation of range and direction between two transceivers is a fundamental problem in array signal processing with applications in radar and wireless localization. In wideband systems, localization performance is fundamentally governed by coherent processing across frequency and antenna dimensions [1]. For example, UWB array processing can jointly estimate direction of arrival (DoA) and time of arrival (ToA) through coherent wideband techniques [2], while space–frequency methods exploit carrier diversity to make range observable together with DoA [3]. However, in many low-cost and low-power radio systems coherent wideband measurement is unavailable, and measurements are instead obtained as narrow-band phase observations across multiple carrier frequencies.

The mathematical framework for distance estimation based on phase measurements at multiple carrier frequencies has been presented in [4], showing that the phase difference between frequencies is linearly proportional to the propagation distance. Algorithms like Multicarrier Phase Difference (MCPD) and FFT-based algorithms have demonstrated centimeter level accuracy on commercial hardware [5], [6]. In multipath-rich environments, techniques such as enhanced MUSIC, orthogonal matching pursuit (OMP), support vector regression (SVR), and atomic norm minimization have been developed to resolve individual paths with improved robustness and computational efficiency [7]–[10].

In parallel, direction estimation using antenna arrays has a long history in radar and communications. Conventional methods range from simple beamforming to high-resolution subspace techniques such as MUSIC and ESPRIT [11]. Other methods such as PDDA, BLUE [12]–[14], provide great angular resolution, but often require strict coherence assumptions, accurate array calibration, and nontrivial computational complexity.

Prior work on joint estimators addresses the variables of interest simultaneously, rather than processing each dimension in sequence, in order to resolve the multiple components present in the received signal. Subspace methods exploit the shift-invariance structure of the space–frequency data, as in the SI-JADE algorithm of [15], alongside maximum-likelihood formulations in [16], [17]. The benefit of joint over sequential processing is further emphasized by estimators that bring in the Doppler dimension. The authors of [18] use a conjugate pair of Zadoff–Chu pilots to first decouple delay and Doppler via maximum likelihood with alternating projections and then refine all parameters together, attaining near-CRB accuracy in dense multipath, while [19] propose a MIMO-OFDM ISAC scheme that DFTs the spatial dimension, cancels symbol-dependent terms through a scaling step, and applies a two-dimensional DFT over fast and slow time to peak-pick in a three-dimensional angle–range–Doppler cube. These methods are designed to separate many overlapping components, whether multipath or distinct targets, which requires their number to be known or estimated and comes at a high computational cost. The present work instead considers a single dominant path, yet still estimates its range and angle jointly rather than one after the other: handling both dimensions together improves accuracy and avoids the error propagation that occurs when one parameter is estimated first and then used to fix the other, all while keeping the procedure simple and computationally light.

We address the problem of joint estimation of range and propagation angle based on the channel impulse response through the measured two-way channel frequency response,

applied to the case of multi-antenna tranceiver. The approach performs joint range and direction estimation by applying a two-dimensional FFT and then searching candidate propagation directions. The measurement method and estimation approach avoid the need for covariance matrix estimation and eigen-decomposition, operating directly on the measured frequency-domain data. The resulting estimator is well suited to low-power wireless systems such as BLE, while remaining broadly applicable to other RF localization scenarios.

II. System Model

The system consists of two radio transceiver units, named Initiator and Reflector, which are positioned r meters apart. The Initiator is equipped with a uniform linear array (ULA) with M antenna elements. The Reflector is assumed to be located in the far-field region of the array such that the planar wavefront approximation is valid. The origin of the coordinate system is in the center of the ULA and the angle θ defines the angle of arrival of the incoming planar wave, as depicted in Figure 1.

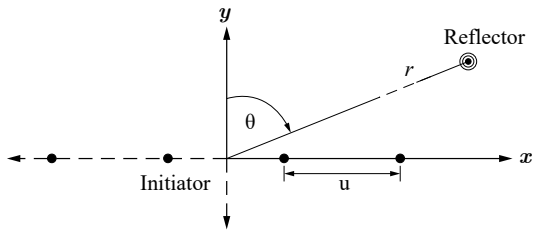

Fig. 1. Setup of the system.

The model follows the Active Reflector principle that has been widely utilized in the literature [5], [6], [8], [20]. Under this model, the initiator and reflector exchange single-tone signals to estimate the bidirectional channel frequency response (CFR), resulting in a two-way CFR measurement. Specifically, the initiator transmits a tone at frequency f_k, selected from a predefined set of K_f channels uniformly spaced at Δ_f. Upon reception, the reflector measures the received phase and responds with a tone at the same frequency while also transmitting the corresponding one-way measured CFR to the Initiator . This exchange enables the initiator with both CFRs. The procedure is repeated over all K_f frequencies and then is carried out sequentially across the antenna elements of the initiator array. As a result, the initiator acquires multichannel CFR measurements across its M antenna elements.

We can express the measurements in the Initiator and Reflector matrices $\mathbf{X}_I, \mathbf{X}_R \in \mathbb{C}^{M\times K_f}$ with entries

$$\mathbf{X}_I = \mathbf{A}(\theta)\mathbf{S}_I(r), \tag{1}$$

$$\mathbf{X}_R = \mathbf{A}(\theta)\mathbf{S}_R(r), \tag{2}$$

where $\mathbf{A}(\theta) \in \mathbb{C}^{M\times K_f}$ is the steering matrix with elements

$$[\mathbf{A}(\theta)]_{m,k} = \exp\left\{ j\,\frac{2\pi k \Delta_f d_m(\theta)}{c} \right\}, \tag{3}$$

where d_m denotes the relative propagation distance at the m-th element with respect to the center of the array. This additional phase rotation is a function of the angle θ, and it is the m-th entry of the vector $\mathbf{d} \in \mathbb{R}^M$, given by

$$\mathbf{d} = \mathbf{P}^T \boldsymbol{\ell}, \tag{4}$$

where $\mathbf{P} = \begin{bmatrix}\mathbf{p}_1 & \dots & \mathbf{p}_M\end{bmatrix} \in \mathbb{R}^{2\times M}$ is the matrix of antenna element positions and the directional cosine unit vector $\boldsymbol{\ell} \in \mathbb{R}^2$ is defined as

$$\boldsymbol{\ell} = \begin{bmatrix}\sin\theta \\ \cos\theta\end{bmatrix}. \tag{5}$$

The matrices $\mathbf{S}_I, \mathbf{S}_R \in \mathbb{C}^{K_f\times K_f}$ are diagonal with $\mathbf{S}_I(r) = \mathrm{diag}(\mathbf{s}_I(r))$ and $\mathbf{S}_R(r) = \mathrm{diag}(\mathbf{s}_R(r))$ with elements

$$[\mathbf{s}_I]_k = b_{I,k}\exp\Big\{ j\Big(\tfrac{2\pi k\Delta_f r}{c} + \Delta\phi_k\Big)\Big\}, \tag{6}$$

$$[\mathbf{s}_R]_k = b_{R,k}\exp\Big\{ j\Big(\tfrac{2\pi k\Delta_f r}{c} - \Delta\phi_k\Big)\Big\}, \tag{7}$$

where $b_{I,k}$ and $b_{R,k}$ denote the amplitudes at the k-th frequency. We assume an ideal, angle independent amplitude response for all elements in the array. The first term in the exponentials of (6) and (7) captures the phase shift induced by the range r. The unknown phase term $\Delta\phi_k$ accounts for both small epoch misalignments between the transceivers and the phase offset arising from their local oscillators.

Under an additive Gaussian noise model, the received measurements at the Initiator and Reflector are given by

$$\mathbf{Y}_I = \mathbf{X}_I + \mathbf{W}_I, \tag{8}$$

$$\mathbf{Y}_R = \mathbf{X}_R + \mathbf{W}_R, \tag{9}$$

where $\mathbf{Y}_I, \mathbf{Y}_R \in \mathbf{C}^{M\times K_f}$ denote the observed measurement matrices, and $\mathbf{X}_I$ and $\mathbf{X}_R$ represent the corresponding noise-free signal components. The noise matrices $\mathbf{W}_I, \mathbf{W}_R \in \mathbb{C}^{M\times K_f}$ consist of independent and identically distributed circularly symmetric complex Gaussian entries with zero mean and variance σ^2, i.e., $[\mathbf{W}_I]_{m,k}, [\mathbf{W}_R]_{m,k} \sim \mathcal{CN}(0,\sigma^2)$.

We take the Hadamard product between the Initiator and Reflector matrices to remove the $\Delta\phi_k$ term in (6) and (7) as showed in [7], [8]. The operation results in the two-way CFR and allows a system with arbitrary phases on each carrier mimic a coherent one. The Hadamard product is defined as

$$\mathbf{Y} \triangleq \mathbf{Y}_I \odot \mathbf{Y}_R, \tag{10}$$

where $\odot$ denotes element-wise multiplication. The (m,k)-th entry of $\mathbf{Y}$ is given by

$$[\mathbf{Y}]_{m,k} = b_{m,k}^2\exp\Big\{ j\Big(\tfrac{4\pi k\Delta_f r}{c} + \tfrac{4\pi k\Delta_f d_m}{c}\Big)\Big\} + W_{m,k}. \tag{11}$$

We assume a static channel during the Initiator-Reflector exchange, so forward and reverse links experience identical propagation-induced amplitudes; hence b_k^2. The term $W_{m,k}$ is the two way noise term, and can be expanded as

$$W_{m,k} \approx X_{R\,m,k}W_{I\,m,k} + X_{I\,m,k}W_{R\,m,k} + W_{I\,m,k}W_{R\,m,k}. \tag{12}$$

As a consequence, the effective noise in the two-way CFR cannot be accurately modeled as additive white Gaussian noise (AWGN). First, the noise statistics depend on the frequency- and antenna-dependent channel responses, which generally vary across the measurement matrix, rendering the noise non-white. Second, the presence of multiplicative terms involving products of Gaussian random variables implies that the resulting noise is no longer Gaussian. Therefore, even if the original one-way noise matrices are modeled as i.i.d. AWGN, the noise induced by the Hadamard product exhibits colored and non-Gaussian characteristics [9].

III. Proposed Estimator

Following the approach in [6], the inverse Fourier transform of the measured CFR is used to obtain a time-domain impulse response, whose delay axis is directly related to the range. In contrast to [6], where a single CFR is processed, we apply the inverse FFT across columns of the measurement matrix (11), resulting in one impulse response per antenna element. The location of the dominant peak in the impulse response corresponds to the propagation delay of the channel, which can be mapped to the range via a linear relationship determined by the frequency sampling and the number of FFT bins. To additionally exploit spatial information, we perform a DFT across the antenna dimension.

We define the IDFT matrix in the frequency dimension as

$$\left[\mathbf{F}_K^H\right]_{k,n} = \frac{1}{N_r} e^{j2\pi kn/N_r}, \quad \begin{matrix} k = 0, \ldots, K_f - 1, \\ n = 0, \ldots, N_r - 1, \end{matrix} \tag{13}$$

and the spatial DFT matrix as

$$\left[\mathbf{F}_M\right]_{p,m} = e^{-j\,2\pi pm/N_\theta}, \quad \begin{matrix} p = 0, \ldots, N_\theta - 1, \\ m = 0, \ldots, M - 1, \end{matrix} \tag{14}$$

where N_r and N_θ are the (zero-padded) IDFT and spatial DFT lengths.

With these definitions, the delay–beamspace representation of the measurements is obtained by applying the IDFT across frequency and the DFT across the antenna dimension of (10) as

$$\mathbf{Z} = \mathbf{F}_M \, \mathbf{Y} \, \mathbf{F}_K^H. \tag{15}$$

The dominant peak in the matrix $\mathbf{Z}$ provides a coarse initial estimate for the joint range–angle parameters. The corresponding delay and spatial frequency indices are obtained as

$$(p_0, n_0) = \arg\max_{p,n} \left|\mathbf{Z}(p,n)\right|. \tag{16}$$

A coarse range estimate is then given by

$$\hat{r}_0 = \frac{c}{2} \frac{n_0}{N_r \Delta f}, \tag{17}$$

where N_r denotes the number of IDFT bins and Δf is the frequency spacing. Similarly, the coarse angle estimate is obtained from the spatial frequency index as

$$\hat{\theta}_0 = \arcsin\left(\frac{\lambda}{2u} \frac{p_0}{N_\theta}\right), \tag{18}$$

where N_θ denotes the number of spatial DFT bins, λ is the wavelength at the central frequency, and u represents the inter-element spacing of the array. For the considered ULA with $M = 16$ elements and inter-element spacing $u = 0.05$ m, the physical angular resolution is approximately $\Delta\theta \approx \frac{\lambda}{Mu} \approx 9^\circ$. In contrast, the FFT grid resolution is $\Delta\theta \approx \frac{\lambda}{2uN_\theta}$ ($\approx 0.03^\circ$ for $N_\theta = 2048$), indicating that the estimation accuracy is limited by the array aperture rather than the discretization grid.

In order to improve the angular resolution, a further search is applied on the delay bin n_0, using the coarse angular estimate $\hat{\theta}_0$ as an initial value. Let $\tilde{\theta} \in \Theta$ denote a hypothesized direction over the search grid $\Theta \subset [-\pi/2, \pi/2]$, and let

$$\mathbf{f}_1 \triangleq \left[\mathbf{Y}\mathbf{F}_K^H\right]_{[:,n_0]}, \tag{19}$$

and $\mathbf{g}(\tilde{\theta}) \in \mathbb{C}^{M\times 1}$ an alignment steering vector with elements

$$[\mathbf{g}(\tilde{\theta})]_m = \exp\left\{-j \, \frac{4\pi k \Delta_f d_m(\tilde{\theta})}{c}\right\}. \tag{20}$$

The estimate is the value $\hat{\theta}$ that maximizes the coherent sum

$$\hat{\theta} = \arg\max_{\tilde{\theta}\in\Theta} \left|\mathbf{g}^T \, \mathbf{Y} \, \mathbf{f}_1\right| \tag{21}$$

while the delay estimate $\hat{n} = n_0$ is retained from the coarse stage.

Intuitively, when the hypothesized direction matches the true direction, the spatial phase compensation aligns the impulse responses across antenna elements, resulting in a maximal coherent peak. The optimal value of $\hat{\theta}$ is found by a gradient ascent on the squared magnitude. Let the objective function be

$$J(\tilde{\theta}) = \left|V(\tilde{\theta})\right|^2, \tag{22}$$

where

$$V(\tilde{\theta}) = \mathbf{g}^T \, \mathbf{Y} \, \mathbf{f}_1 \; = \sum_{m,k} Y_{m,k} e^{-j\frac{4\pi k\Delta_k}{c} d_m(\tilde{\theta})} e^{j\frac{2\pi k n_0}{N_r}}. \tag{23}$$

Let

$$\Phi_{m,k}(\tilde{\theta}) = \frac{4\pi k \Delta_f}{c} \, d_m(\tilde{\theta}), \tag{24}$$

and

$$\frac{\partial \Phi_{m,k}}{\partial \tilde{\theta}} = \frac{4\pi k \Delta_f}{c} \, \frac{\partial d_m(\tilde{\theta})}{\partial \tilde{\theta}}. \tag{25}$$

The derivative of $V(\tilde{\theta})$ with respect of $\tilde{\theta}$ is

$$\frac{dV}{d\tilde{\theta}} = \sum_{m,k} Y_{m,k} \left(-j \frac{\partial \Phi_{m,k}}{\partial \tilde{\theta}}\right) e^{-j\Phi_{m,k}(\tilde{\theta})} e^{j\frac{2\pi k n_0}{N_r}}. \tag{26}$$

TABLE I
SIMULATION PARAMETERS USED IN THE MONTE–CARLO EVALUATION

Parameter	Symbol	Value
Number of frequency bins	K_f	77
Frequency spacing	Δ_f	1 MHz
Speed of light	c	2.9979×10^8 m/s
Number of array elements	M	16
Element spacing	u	0.05 m
IFFT bins	N_r	2048
FFT bins	N_θ	2048
SNR range	SNR	$[-10, 10]$ dB
Number of Monte–Carlo trials	N_{trials}	20000

Using $J(\tilde{\theta}) = V(\tilde{\theta})V^*(\tilde{\theta})$, the derivative of the objective becomes

$$\frac{dJ}{d\tilde{\theta}} = 2\,\Re\left\{\frac{dV}{d\tilde{\theta}}\,V^*(\tilde{\theta})\right\}, \tag{27}$$

and the iterate is updated as

$$\tilde{\theta}^{(i+1)} = \tilde{\theta}^{(i)} + \mu\,\frac{dJ}{d\tilde{\theta}}\bigg|_{\tilde{\theta}^{(i)}}, \qquad \tilde{\theta}^{(0)} = \hat{\theta}_0, \tag{28}$$

with $\hat{\theta} = \tilde{\theta}^{(N_\text{i})}$ taken as the final estimate after N_i iterations.

In noise ratios above 0dB, for a defined step size of $\delta_s = 10^{-5}$ and for a number of 30 iterations the gradient magnitude decreases to approximately 10^{-4} which we consider sufficient for convergence.

In terms of computational complexity, computing the delay impulse responses with the IFFT for all antenna elements has a complexity $\mathcal{O}(MN_r \log N_r)$. After retaining the nonnegative delays, the spatial FFT has complexity $\mathcal{O}(N_\theta N_r \log N_\theta)$. The peak search over the delay–beamspace map requires $\mathcal{O}(N_\theta N_r)$, which is negligible compared to the FFT stages. The optional gradient-based refinement step operates directly on the measured frequency samples and has per-iteration complexity $\mathcal{O}(MK_f)$. Since the number of refinement iterations is small and fixed, its overall contribution remains moderate.

IV. NUMERICAL RESULTS

In order to test the behavior of the proposed IFFT-based estimator we have run simulations using the parameters commonly used by BLE radios and are given in Table I.

The performance of the estimator is assessed in terms of mean squared error (MSE) and compared against the corresponding genie-aided Cramér–Rao lower bounds i.e. a bound for each parameter assuming perfect knowledge of the other parameter. These can be considered optimistic for the joint estimation problem. The CRLB for range [21] is adjusted in SNR to account for the array gain introduced by the M-element ULA in the proposed estimator, and is given by

$$\text{CRLB}_r = \frac{3c_0^2}{4M\gamma\pi^2\Delta_f^2 K_f\left(K_f^2 - 1\right)}, \tag{29}$$

where γ denotes the signal-to-noise ratio (SNR) defined as $\frac{|b_{m,k}^2|}{\sigma^2}$.

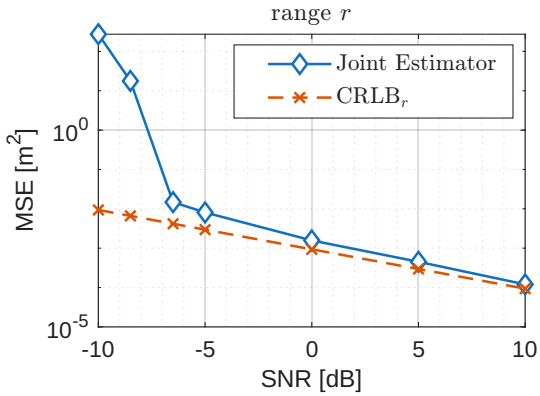

Fig. 2. MSE for range estimation

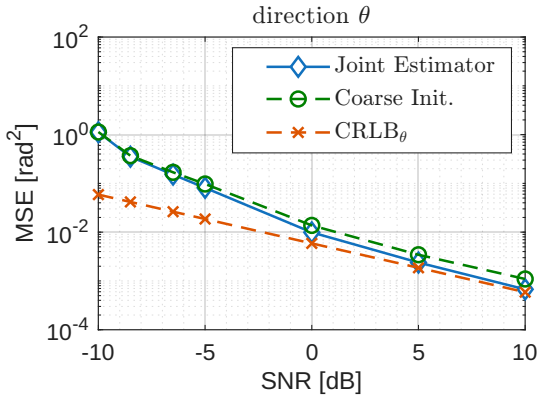

Fig. 3. MSE for angle estimation

The CRLB for direction-of-arrival estimation is derived from [11]. Its variance expression has been adapted to account for the two-way CFR model used in our formulation. The resulting bound is

$$\text{CRLB}_\theta = \frac{24}{\gamma\, M(M^2-1)}. \tag{30}$$

From Figure 2, it can be observed that the MSE of the range estimate approaches the CRLB at approximately -5 dB SNR. As expected, the estimation error decreases monotonically with increasing SNR.

A similar behavior is observed for the angular estimate in Figure 3. The MSE of $\hat{\theta}$ approaches the corresponding CRLB at approximately 0 dB SNR, indicating efficient performance in the moderate-to-high SNR regime. The FFT based coarse angle estimate is surprisingly accurate, but does not approach the CRLB, while the gradient search is able to improve the performance approaching the bound.

The residual gaps between the simulated MSEs and the bounds in the high-SNR regime can be attributed to two main factors. Firstly, discretization effects introduced by the finite DFT grid lead to quantization errors in both the delay and angular domains. Secondly, the CRLB expressions employed are adapted bounds derived under simplifying assumptions. In particular, they do not correspond to the joint Fisher

information of the coupled range–angle estimation problem considered here, but instead assume knowledge of the remaining parameters. As a result, the bounds are expected to be optimistic.

V. Conclusion

In this paper, we proposed an FFT-based joint range and angle estimator for BLE-like systems based on delay-beamspace processing of the measured two-way channel frequency response. By combining an IDFT across frequency with a spatial DFT across antenna elements, the proposed method enables coherent integration in both delay and angular domains while maintaining low computational complexity.

The proposed system is able to estimate both range and propagation angle despite the fact that two way phase measurement includes arbitrary phase offsets between different frequencies and antennas. The algorithm provides joint range-angle estimation with near-optimal statistical performance at moderate and high SNRs while preserving the computational efficiency of standard FFT-based processing, making it suitable for low-power embedded implementations such as BLE devices.

Acknowledgment

The work is supported by the Research Council of Norway through the Phased-array radio systems for resilient localization and navigation of autonomous systems in GNSS-denied environments (PARNAV) project (No. 338789).

References

[1] C. Gentile, A. J. Braga, and A. Kik, "A Comprehensive Evaluation of Joint Range and Angle Estimation in Ultra-Wideband Location Systems for Indoors," in *2008 IEEE International Conference on Communications*, May 2008, pp. 4219–4225. [Online]. Available: https://ieeexplore.ieee.org/document/4533828

[2] A. Ramírez-Arroyo, A. Alex-Amor, P. Padilla, and J. F. Valenzuela-Valdés, "Joint Direction-of-Arrival and Time-of-Arrival Estimation With Ultra-Wideband Elliptical Arrays," *IEEE Transactions on Wireless Communications*, vol. 22, no. 12, pp. 9187–9200, Dec. 2023. [Online]. Available: https://ieeexplore.ieee.org/document/10109651/citations

[3] Z. Mao, S. Liu, Y. D. Zhang, L. Han, and Y. Huang, "Joint DoA-Range Estimation Using Space-Frequency Virtual Difference Coarray," *IEEE Transactions on Signal Processing*, vol. 70, pp. 2576–2592, 2022. [Online]. Available: https://ieeexplore.ieee.org/document/9770366

[4] M. Pelka, C. Bollmeyer, and H. Hellbrück, "Accurate radio distance estimation by phase measurements with multiple frequencies," in *2014 International Conference on Indoor Positioning and Indoor Navigation (IPIN)*, Oct. 2014, pp. 142–151. [Online]. Available: https://ieeexplore.ieee.org/document/7275478

[5] P. Zand, J. Romme, J. Govers, F. Pasveer, and G. Dolmans, "A high-accuracy phase-based ranging solution with Bluetooth Low Energy (BLE)," in *2019 IEEE Wireless Communications and Networking Conference (WCNC)*, Apr. 2019, pp. 1–8. [Online]. Available: https://ieeexplore.ieee.org/document/8885791

[6] Y. Schröder, D. Reimers, and L. Wolf, "Accurate and Precise Distance Estimation from Phase-Based Ranging Data," in *2018 International Conference on Indoor Positioning and Indoor Navigation (IPIN)*, Sep. 2018, pp. 1–8. [Online]. Available: https://ieeexplore.ieee.org/document/8533871

[7] P. Boer, J. Romme, J. Govers, and G. Dolmans, "Performance of High-Accuracy Phase-Based Ranging in Multipath Environments," in *2020 IEEE 91st Vehicular Technology Conference (VTC2020-Spring)*, May 2020, pp. 1–5. [Online]. Available: https://ieeexplore.ieee.org/document/9128721

[8] S. N. Shoudha, J. P. Van Marter, S. Helwa, A. G. Dabak, M. Torlak, and N. Al-Dhahir, "Reduced-Complexity Decimeter-Level Bluetooth Ranging in Multipath Environments," *IEEE Access*, vol. 10, pp. 38 335–38 350, 2022, conference Name: IEEE Access. [Online]. Available: https://ieeexplore.ieee.org/document/9751073

[9] J. P. Van Marter, A. G. Dabak, N. Al-Dhahir, and M. Torlak, "Support Vector Regression for Bluetooth Ranging in Multipath Environments," *IEEE Internet of Things Journal*, vol. 10, no. 13, pp. 11 533–11 546, Jul. 2023, conference Name: IEEE Internet of Things Journal. [Online]. Available: https://ieeexplore.ieee.org/document/10044207

[10] A. Sheikh, J. Romme, J. Govers, A. Farsaei, and C. Bachmann, "Phase-Based Ranging in Narrowband Systems With Missing/Interfered Tones," *IEEE Internet of Things Journal*, vol. 10, no. 17, pp. 15 171–15 185, Sep. 2023, conference Name: IEEE Internet of Things Journal. [Online]. Available: https://ieeexplore.ieee.org/document/10092848

[11] P. Stoica and A. Nehorai, "MUSIC, maximum likelihood, and Cramer-Rao bound," *IEEE Transactions on Acoustics, Speech, and Signal Processing*, vol. 37, no. 5, pp. 720–741, May 1989. [Online]. Available: https://ieeexplore.ieee.org/document/17564/

[12] M. A. G. Al-Sadoon, N. T. Ali, Y. Dama, A. Zuid, S. M. R. Jones, R. A. Abd-Alhameed, and J. M. Noras, "A New Low Complexity Angle of Arrival Algorithm for 1D and 2D Direction Estimation in MIMO Smart Antenna Systems," *Sensors*, vol. 17, no. 11, p. 2631, Nov. 2017. [Online]. Available: https://www.mdpi.com/1424-8220/17/11/2631

[13] H. Ye, B. Yang, Z. Long, and C. Dai, "A Method of Indoor Positioning by Signal Fitting and PDDA Algorithm Using BLE AOA Device," *IEEE Sensors Journal*, vol. 22, no. 8, pp. 7877–7887, Apr. 2022, conference Name: IEEE Sensors Journal. [Online]. Available: https://ieeexplore.ieee.org/document/9676583

[14] C. Huang, J. Li, and H. Liu, "A Closed-Form Phase Difference Estimation Method for BLE Direction Finding using the Best Linear Unbiased Estimator," in *2023 IEEE 23rd International Conference on Communication Technology (ICCT)*, Oct. 2023, pp. 1048–1052. [Online]. Available: https://ieeexplore.ieee.org/document/10419676

[15] A.-J. Van Der Veen, M. Vanderveen, and A. Paulraj, "Joint angle and delay estimation using shift-invariance techniques," *IEEE Transactions on Signal Processing*, vol. 46, no. 2, pp. 405–418, Feb. 1998. [Online]. Available: http://ieeexplore.ieee.org/document/655425/

[16] A. Bazzi, D. T. M. Slock, and L. Meilhac, "Efficient Maximum Likelihood Joint Estimation of Angles and Times of Arrival of Multiple Paths," in *2015 IEEE Globecom Workshops (GC Wkshps)*. San Diego, CA, USA: IEEE, Dec. 2015, pp. 1–7. [Online]. Available: http://ieeexplore.ieee.org/document/7414203/

[17] F. Bellili, S. B. Amor, S. Affes, and A. Ghrayeb, "Maximum Likelihood Joint Angle and Delay Estimation from Multipath and Multicarrier Transmissions with Application to Indoor Localization over IEEE 802.11ac Radio," *IEEE Transactions on Mobile Computing*, vol. 18, no. 5, pp. 1116–1132, May 2019. [Online]. Available: https://ieeexplore.ieee.org/document/8410008/

[18] Z. Yang, R. Wang, Y. Jiang, and J. Li, "Joint Estimation of Velocity, Angle-of-Arrival and Range (JEVAR) Using a Conjugate Pair of Zadoff-Chu Sequences," *IEEE Transactions on Signal Processing*, vol. 69, pp. 6009–6022, 2021. [Online]. Available: https://ieeexplore.ieee.org/document/9591345/

[19] Z. Xiao, R. Liu, M. Li, Q. Liu, and A. L. Swindlehurst, "A Novel Joint Angle-Range-Velocity Estimation Method for MIMO-OFDM ISAC Systems," *IEEE Transactions on Signal Processing*, vol. 72, pp. 3805–3818, 2024. [Online]. Available: https://ieeexplore.ieee.org/document/10634583/

[20] K. Kansanen, J. A. Forbord, and J. Suárez, "Bayesian Distance Estimation with Incoherent Multi-Frequency Two-Way Phase Measurements," in *2025 33rd European Signal Processing Conference (EUSIPCO)*, Sep. 2025, pp. 1972–1976. [Online]. Available: https://ieeexplore.ieee.org/document/11226184/

[21] D. Maklada, Y. Obeid-Zoabi, A. Eilam, and M. Dikshtein, "High Accuracy Distance Measurement Using Frequency Comb," in *2021 IEEE International Conference on Microwaves, Antennas, Communications and Electronic Systems (COMCAS)*, Nov. 2021, pp. 361–366. [Online]. Available: https://ieeexplore.ieee.org/document/9629073